The Journal of Medicinal Plants and By-Products

Original Article

Fabrication of *Pistacia atlantica* Oil-Encapsulated Chitosan Nanoparticles in Polyvinyl Alcohol Nanofibers: Biocompatibility and Antioxidant Properties for Skin Care Applications

Running Title: Pistacia Oil-Loaded Nanoparticles in PVA Nanofibers

Vahid Ghotbi Maleki[1], Faezeh Fathi[1], Hossein Behboudi[2], Nezam Armand[3] and Samad Nejad Ebrahimi[1,*]

[1] *Department of Phytochemistry, Medicinal Plants and Drugs Research Institute, Shahid Beheshti University, Tehran, Iran*
[2] *Department of Biology, Medicinal Plants and Drugs Research Institute, Shahid Beheshti University, Tehran, Iran*
[3] *Evidence-based Phytotherapy and Complementary Medicine Research Center, Alborz University of Medical Sciences, Karaj, Iran*

*Corresponding author: Email: s_ebrahimi@sbu.ac.ir

Article History: Received: 07 December 2024/Accepted in revised form: 29 December 2024

ABSTRACT

This study provides a comprehensive nutritional and phytochemical analysis of *Pistacia atlantica* fruit (PAF), which revealed a high fat content (33.90%) and carbohydrate content (62.41%), identifying it as a significant energy source. Phytochemical profiling demonstrated notable levels of phenolics (17.70 ± 1.59 mg GAE/g dry weight) and flavonoids (6.46 ± 0.35 mg CE/g), contributing to substantial antioxidant properties. A novel nanocomposite was developed by encapsulating *Pistacia atlantica* oil (PAO) within chitosan nanoparticles (CNPs) using ionic gelation with sodium tripolyphosphate, followed by embedding these nanoparticles into polyvinyl alcohol (PVA) nanofibers. Characterization of the resulting nanocomposite revealed a mean particle size of 104.76 nm and a polydispersity index (PDI) of 0.41, indicating a uniform size distribution. The encapsulation efficiency (EE%) of PAO was consistent across formulations, while the loading capacity (LC%) increased with higher CNP content, achieving a maximum of 32.37% for a PVA ratio of 1:2. Antioxidant assays confirmed robust activity, with FRAP and DPPH values of 79.4 ± 2.1 µmol ESF/100g and an IC_{50} of 7344.7 µg/mL, respectively. Cell viability assays demonstrated excellent biocompatibility, with CNP and PVA-CNP formulations maintaining over 82% viability in human dermal fibroblast cells. The CNP-PVA nanofiber system infused with PAO demonstrates controlled release, robust antioxidant properties, and superior biocompatibility, positioning it as a potential solution for wound healing and skin care needs.

Keywords: *Pistacia atlantica*, Chitosan nanocapsules, PVA nanofibers, Antioxidant, Wound healing, Biocompatibility

INTRODUCTION

Natural products and herbal extracts have long played a vital role in promoting skin health and supporting wound healing. The incorporation of bioactive compounds derived from plants has been shown to significantly accelerate the wound-healing process through mechanisms such as reducing inflammation, enhancing collagen synthesis, and providing potent antioxidant protection. Together, these actions facilitate effective tissue repair and regeneration, making such formulations valuable for treating both minor skin injuries and more severe wounds. The efficacy of these natural agents is largely attributed to their antioxidant and anti-inflammatory properties, particularly due to the presence of polyphenolic compounds, which have consistently demonstrated therapeutic benefits. [1-3].

Among medicinal plants, *Pistacia atlantica*, commonly known as the Atlas pistachio, stands out for its rich phytochemical composition and remarkable health benefits. The seed oil of *Pistacia atlantica* is particularly rich in antioxidants, which protect the skin from oxidative stress and promote wound healing. Historically, this plant has been employed to manage a range of conditions, such as hypertension, diabetes, and infections, attributed to its wide array of biological effects, including antibacterial, antifungal, and anti-inflammatory properties [4-7]. Specifically, the oil's ability to modulate inflammation and stimulate tissue regeneration highlights its potential in wound management [8, 9].

he biochemical profile of *P. atlantica* oil highlights its richness in essential compounds, including fatty acids, sterols, and tocopherols, with gas chromatography (GC) commonly employed for their identification. The oil's favorable unsaturated-to-saturated fatty acid ratio, primarily composed of oleic and linoleic acids, underscores its therapeutic potential. These fatty acids are essential for supporting reepithelialization and encouraging neovascularization throughout the healing process, reinforcing the oil's value in both skincare and clinical wound management [6, 8, 10, 11]. Additionally, formulations based on *P. atlantica* oil, such as gels, have shown efficacy in reducing wound size and facilitating collagen synthesis, further validating their medicinal value [12, 13].

To enhance the stability, bioavailability, and controlled release of herbal extracts and oils, advanced encapsulation techniques, such as microencapsulation and nanoencapsulation, are increasingly employed. Methods including

emulsification, ionic gelation, coacervation, and nanoprecipitation provide protection against degradation while improving the solubility of hydrophobic compounds. Encapsulation using biocompatible materials, such as chitosan and alginate, not only safeguards these bioactive ingredients but also extends their shelf life, the highly adaptable for use in food, pharmaceutical, and cosmetic formulations [14-16]. These advancements enable the development of innovative delivery systems that enhance the functional benefits of natural products, offering substantial potential for the cosmetic and pharmaceutical sectors [17-21].

Electrospinning technology has emerged as an effective method for incorporating herbal extracts and oils into polymeric nanofibers, enhancing wound healing and skin protection. This technique is especially valued for its cost-efficiency and its ability to produce continuous nanofibers with a large surface area, which enhances drug delivery and improves the functionality of wound dressings [22, 23]. The incorporation of bioactive agents, such as *Carica papaya* extracts, into these nanofibers has proven effective for wound care applications [24]. Furthermore, the addition of components like gold nanoparticles expands the antimicrobial and healing capabilities of these nanofiber composites, showcasing the versatility and promise of electrospun materials in medical and therapeutic contexts [25, 26].

In this work, we selected *P. atlantica* oil for its rich phytochemical composition and therapeutic potential in promoting wound healing and skin protection. Additionally, electrospinning technology was chosen for its cost-efficiency and ability to effectively incorporate this oil into polymeric nanofibers, enhancing its therapeutic benefits as a natural antioxidant and skincare agent.

MATERIAL AND METHODS

Chemicals and Reagents

Polysorbate 80 (Extra Pure) from Neutron (Tehran, Iran) and chitosan (medium molecular weight, 85% deacetylation) were obtained from Sigma-Aldrich and subsequently cross-linked with sodium tripolyphosphate (TPP) from Merck to fabricate nanocapsule structures. Polyvinyl alcohol (PVA with a molecular weight of 72,000 and a minimum degree of hydrolysis of 99%.) was sourced from Merck. Ethanol, methanol, and hexane (analytical grade, 99% purity; Sigma-Aldrich) were used for extraction, while phosphate-buffered saline (PBS) and additional buffer solutions were prepared using reagent-grade chemicals from Thermo Fisher. Antioxidant assay reagents, including DPPH and FRAP, were obtained from the reputable supplier Sigma-Aldrich, while the essential chemicals for fatty acid esterification, pivotal for GC-MS analysis, were sourced from reliable providers.

Plant Material

P. atlantica fruits (PAF) were sourced from a local market in Kermanshah, Iran, during September and October 2020. The fruits underwent thorough washing with distilled water, were carefully cleaned, and dried at a temperature of 25 °C. They were then ground into a fine powder for analysis.

Nutritional Profile of PAF

The nutritional composition of *P. atlantica* fruits (PAF) was assessed using standardized procedures to determine moisture, protein, ash, fat, and carbohydrate levels. Moisture content analysis was performed in triplicate using an infrared moisture analyzer operated at 105 °C (DBS-KERN & SOHN GmbH, DBS60-3, Balingen, Germany), and the results were expressed per 100 g of dried seeds [27]. The Kjeldahl method was employed to determine the total protein content, with acid digestion performed for one hour in an automated digester (K-438, Buchi®, Switzerland), adhering to the AOAC 992.15 protocol [27]. Ammonia was released from the digested sample by adding 90 mL of 32% NaOH, distilled, and captured in 60 mL of 4% boric acid at a pH of 4.65. The solution was then titrated with 0.2 M H_2SO_4 using methyl red as an indicator. The total protein content was determined by converting the total nitrogen with a factor of 6.25, and the results were reported per 100 g of dried PAF [27, 28]. The analysis of ash content involved heating PAF in a muffle furnace (Thermolyne 48000, Electrothermal Engineering Ltd., Essex, UK) at 500 °C until the residue turned into white ash, in accordance with standard procedures. The experiment was carried out in triplicate, and the findings were reported in grams per 100 g of dried fruit [27]. The Soxhlet method was utilized to evaluate the total fat content through continuous extraction (AOAC 991.36), with the results expressed as grams of fat per 100 g of dried PAF [27]. All analyses were conducted in triplicate to ensure reliability.

The available carbohydrate content was calculated using the formula:

Available carbohydrates (%) = 100 − (% moisture + % protein + % fat + % ash)

The results were expressed in grams per 100 g of dried seeds.

Antioxidant Capacity of PAF Extract:

Extract Preparation

Extracts were prepared by incubating 500, 250, and 125 mg of dried and ground PAF in 50 mL of a 50:50 ethanol/water solution at 40 °C for 1 hour with continuous agitation. The extraction process, performed in triplicate, involved filtering the

solutions and storing them at -20 °C for subsequent analysis. Spectrophotometric methods were used to determine the total phenolic and flavonoid content of the extracts, along with their antioxidant capacity [28].

Total Phenolic Content

Phenolic content was assessed by mixing 30 µL of extract with 150 µL of Folin-Ciocalteu reagent and 120 µL of 7.5% sodium carbonate. The mixture was incubated at 45 °C for 15 minutes and left in the dark at room temperature for 30 minutes. Absorbance at 765 nm was measured using a BioTek spectrophotometer (Synergy HT). Gallic acid served as the standard (5–100 mg/mL; $y = 0.0097x + 0.0154$, $R^2 = 0.9977$). Results, averaged from triplicates, were expressed as milligrams of gallic acid equivalents (GAE) per gram of dried PAF.

Total Flavonoid Content

Flavonoid content was measured by diluting 1 mL of extract with 4 mL of water, mixing with 300 µL of 5% sodium nitrate, and allowing a 5-minute reaction. After adding 300 µL of 10% aluminum chloride, 2 mL of 1M sodium hydroxide, and 2.5 mL of water, absorbance was recorded at 510 nm. Catechin was the standard (0–400 µg/mL; $y = 0.002x + 0.0062$, $R^2 = 0.9983$). Results, expressed as milligrams of catechin equivalents per gram of dried PAF, were averaged from triplicates.

FRAP and DPPH Assays

The FRAP assay involved reacting 35 µL of extract with 265 µL of FRAP reagent (0.3 M acetate buffer, 10 mM TPTZ, 20 mM ferric chloride) at 37 °C for 30 minutes in the dark. Absorbance was recorded at 595 nm, with ferrous sulfate as the standard (0–600 µg/mL; $y = 0.0024x + 0.0005$, $R^2 = 0.9991$). Results were expressed as micromoles of ferrous sulfate equivalents (FSE) per gram of dried PAF.

For DPPH radical scavenging, 30 µL of extract was combined with 270 µL of ethanolic DPPH solution, and absorbance was monitored at 525 nm over 40 minutes. Trolox was the standard (5.62–175.34 µg/mL; $y = -0.0068x + 0.5605$, $R^2 = 0.9995$), and results were expressed as milligrams of Trolox equivalents (TE) per gram of dried seeds based on triplicate readings.

Extraction of PAO

PAO was obtained by cold pressing at 25 °C. A 1000-gram sample was pressed using a hydraulic press (Iran Cold Press 65MM) at 16 kg/cm² for 60 minutes without added heat. The oil was left to settle for one week to separate solids, then filtered and kept at 4 °C [29].

Fatty Acid Methyl Ester Preparation

Fatty acid methyl esters (FAME) were prepared from the hexane extract through saponification and esterification. A mixture of 10 mg of oil, 0.5 mL of n-hexane, and 2 mL of 2 M potassium hydroxide in methanol was vortexed for 2 minutes and heated at 60 °C for 15 minutes. After cooling, 2 mL of 20% NaCl and 0.5 mL of n-hexane were added, followed by vortexing and centrifugation for 10 minutes. The upper phase (1 µL) was subjected to analysis using GC-FID and GC-MS.

Fatty Acid Composition Analysis

The fatty acid composition of *P. atlantica* oil (PAO) was analyzed following a previously described esterification method. The analysis utilized a ThermoQuest-Finnigan gas chromatograph with a flame ionization detector (FID) and a DB-5 capillary column (30 m × 0.25 mm, 0.25 µm film thickness). Nitrogen was employed as the carrier gas, using a split ratio of 1:10. Injector and detector temperatures were set at 280 °C. The column temperature program began at 60 °C for 38 minutes, increased at a rate of 5 °C/min to 250 °C, and was held at 250 °C for 2 minutes.

Formulation of Electrospinning Solutions

Chitosan was used to encapsulate PAO via ionic gelation, adapting a method by Ahmadi et al. (2018). Chitosan (1 g) was dissolved in 100 mL of 1% acetic acid solution with continuous stirring until fully solubilized. To this solution, 1% Tween 80 was added as an emulsifier, and stirring was continued for 1 hour. Subsequently, 1000 µL of PAO was added dropwise, followed by sonication at 60% power for 5 minutes (5-second intervals on and off) using a 100 kW probe sonicator. The mixture was then stirred at 500 rpm for an additional hour. For cross-linking, 0.5 g of tripolyphosphate (TPP) was dissolved in 100 mL of water and slowly introduced into the PAO/chitosan/Tween 80 emulsion under continuous stirring at 1000 rpm. The mixture was then subjected to sonication to ensure proper cross-linking. The resulting cloudy solution was stirred overnight to ensure uniformity. Chitosan nanocapsules (CNP) were separated by centrifugation at 4000 × g for 5 minutes.

Electrospinning solutions were prepared by mixing a 10% polyvinyl alcohol (PVA) solution with CNP at different ratios (0.25:1, 0.5:1, 1:1, and 1:0.5). The mixtures were sonicated and stirred for 30 minutes to achieve homogeneity.

Fiber Formation

The electrospinning process was performed using a Fanavaran Nanomeghyas machine with a single pump. The PVA-CNP polymer mixture was loaded into a 3 mL syringe fitted with a 1.5 mm needle connected to a syringe pump. The needle was positioned 10 cm away from the collector, with a voltage of 15 kV and a flow rate of 0.7 mL/h. Nanofibers were deposited onto aluminum foil affixed to the collector.

Dynamic Light Scattering

The nanocapsule size distribution and polydispersity index (PDI) were assessed by diluting the samples in water (1:20) and creating volume frequency histograms. Measurements were performed using a Nanophox 90-246V device (Germany) at 25 °C and a fixed angle of 173°. All tests were done in triplicate.

Morphology and Fiber Diameter

Scanning electron microscopy (SEM) was used to examine the surface morphology of the nanofibers. The samples were mounted on holders, gold-coated with a sputter coater, and analyzed at room temperature with an acceleration voltage of 25 kV. Images were acquired using a Hitachi SU3500 SEM (Japan).

Fourier Transform Infrared (FT-IR) Spectroscopy

Chemical interactions in the nanocapsules and nanofibers were analyzed using Attenuated total reflectance (ATR)-FTIR spectroscopy (Thermo Nicolet, Madison, WI, USA). Measurements were conducted at room temperature in the transmission mode, spanning a wavelength range of 400–4000 cm^{-1}. Composite nanofibers were dried in a desiccator to confirm the incorporation of PAO into the PVA-chitosan matrix.

Encapsulation Efficiency and Loading Capacity

Encapsulation efficiency (EE) and loading capacity (LC) of the nanocapsules were assessed using UV-Vis spectroscopy (OPTIMA SP-3000 plus, Tokyo, Japan), with PAO exhibiting maximum absorbance at 270 nm. For the analysis, 20 mg of the sample was dissolved in a 2% Tween 80 solution and stirred overnight. Following centrifugation at 3000 × g for 10 minutes, the supernatant was collected for absorbance measurements. A calibration curve was constructed using PAO diluted in ethanol (0.5–5 mg/mL). EE and LC were calculated using the following formula:

EE (%) = [Total loaded oil / Total oil] × 100 (**1**)

LC (%) = [Total loaded oil / Total nanocomposite weight] × 100 (**2**)

Release Study of PAO nanocapsules and nanofibers

In vitro drug release studies of PVA nanofibers loaded with CNP (PCP NFs) were performed following established protocols described in prior research [30, 31], with modifications. Drug release was assessed by immersing 20 mg of nanocomposite fibers in 20 mL of phosphate-buffered saline (PBS) at pH 7.4 (physiological conditions) and pH 5.5 (skin conditions), maintained at 37 °C with shaking at 90 rpm. At predefined time intervals, 2 mL of the medium was withdrawn, centrifuged at 2000 rpm for 5 minutes, and replaced with fresh PBS. This procedure was repeated over a 30-hour period. The concentration of PAO in the collected samples was measured using a UV-Vis spectrophotometer (Shimadzu, model 2051PC, Japan) at 270 nm, using a standard calibration curve for quantification. All experiments were performed in triplicate, with mean values reported.

Antioxidant Capacity of Nanocapsules and Nanofibers

The antioxidant activity of PAO-loaded nanomaterials was analyzed using DPPH and FRAP assays, utilizing a UV-Vis spectrophotometer microplate reader (Epoch2, BioTek, Santa Clara, USA). For the DPPH assay, a 0.1 mM methanolic DPPH solution was freshly prepared as a free radical source. Nanofiber samples were dissolved or dispersed in methanol at specified concentrations. A 100 µL aliquot of the sample solution was mixed with 100 µL of the DPPH solution in a 96-well microplate and incubated in the dark at room temperature for 30 minutes. Absorbance was measured at 517 nm [32]. The antioxidant capacity was evaluated by measuring the change in absorbance and comparing it to a standard curve prepared using ferrous sulfate solutions [33].

In Vitro Cytotoxicity of Nanocapsules and Nanofibers

Human dermal fibroblast (HDF) cells were obtained from the National Cell Bank of Iran (Pasteur Institute, Iran) and cultured in RPMI-1640 medium (Gibco) supplemented with 10% fetal bovine serum (FBS) and antibiotics (100 U/mL penicillin and 100 µg/mL streptomycin). The cells were maintained at 37 °C in a humidified environment with 5% CO_2. Routine cell passaging was conducted using trypsin/EDTA (Gibco) and phosphate-buffered saline (PBS).

Cell viability and proliferation were assessed using the MTT assay [3-(4,5-dimethylthiazol-2-yl)-2,5-diphenyltetrazolium bromide] (Sigma-Aldrich). Cells were trypsinized, adjusted to 1.5×10^4 cells per well, and seeded in 96-well plates with 200 µL of medium, followed by 24 hours of incubation. Test compounds (1000–62.5 µg/mL) were added, and cells were treated for 48 hours at 37 °C under 5% CO_2. After treatment, 200 µL of 0.5 mg/mL MTT solution was added, and plates were incubated at 37 °C for 4 hours. The medium was replaced with 100 µL of DMSO to dissolve formazan crystals, and absorbance was measured at 570 nm using an ELISA reader (Wave XS2, BioTek, USA).

RESULT AND DISCUSSIONS

Nutrients Value Analysis of PAF

The nutritional analysis of *P. atlantica* (Baneh) samples, presented in Table 1, demonstrates that they are rich in essential nutrients, particularly fat and carbohydrates. The samples consist of 5.33% moisture, 2.04% ash, 33.90% fat, 1.65% crude protein, and 62.41% total carbohydrates. The substantial fat content highlights Baneh nuts as a rich energy source, while the high carbohydrate levels indicate their potential for sustained energy release. Furthermore, these nutritional components contribute to therapeutic properties, such as promoting wound healing and enhancing skin protection [34, 35]. The ratio of fat to carbohydrates in *P. atlantica* fruit (PAF) is approximately 1:2, indicating a balanced macronutrient profile. This ratio suggests that the fruit provides a harmonious combination of energy-dense fats and carbohydrates, which can support sustained energy release while maintaining a favorable nutrient balance. Such a profile is beneficial for both nutritional purposes and therapeutic applications, particularly Table 2 presents the bioactive compounds and antioxidant activity of *P. atlantica* fruit (PAF). The results demonstrate that PAF is a rich source of phenolic compounds and flavonoids, both of which are well-known for their potent antioxidant properties. The total phenolic content was quantified as 17.70 ± 1.59 mg gallic acid equivalents (GAE) per gram of dry weight, while the flavonoid content was measured at 6.46 ± 0.35 mg catechin equivalents (CE) per gram of dry weight.

The antioxidant properties of Baneh nuts were assessed through the Ferric Reducing Antioxidant Power (FRAP) and DPPH radical scavenging assays. The FRAP assay revealed significant antioxidant capacity, with a result of 200.99 ± 9.92 µmol ferrous sulfate equivalents (FSE) per gram of dry weight. Similarly, the DPPH assay demonstrated strong activity, yielding 23.81 ± 0.53 mg Trolox equivalents (TE) per gram of dry weight. These results align with prior research on *P. atlantica*, which has shown high levels of phenolic and flavonoid compounds and remarkable antioxidant activity. Moreover, the bioactive potential of PAF extracts and oils underscores their therapeutic value, particularly in skincare and wound healing, where their antioxidant and phenolic content contribute to their effectiveness [12].

Table 1 Nutritional analysis of *Pistacia atlantica* in dry Weight.

Sample	Moisture (%)	Ash	Fat	Crude Protein	Total carbohydrates
Baneh	5.33 ± 0.42	2.04 ± 0.01	33.90 ± 0.57	1.65 ± 0.19	62.41 ± 0.63

The results are presented as mean ± standard deviation, expressed in g/100 g.

Table 2 Bioactive compounds and antioxidant activity of *Pistacia atlantica*.

Sample	Bioactive compounds		Antioxidant activity	
	Total Phenolics	Flavonoids	FRAP	DPPH•
	mg GAE /g	*mg CE /g*	*µmol ESF/g*	*mg TE/g*
Baneh	17.70 ± 1.59	6.46 ± 0.35	200.99 ± 9.92	23.81 ± 0.53

Results are expressed on a dry weight basis as mean ± standard deviation (n= 3). Abbreviations: GAE – Gallic Acid Equivalents; CE – Catechin Equivalents; FRAP – Ferric Reducing Antioxidant Power; FSE – Ferrous Sulphate Equivalents; DPPH• – 2,2-Diphenyl-1-picrylhydrazyl radical; TE – Trolox Equivalents

Table 3 Fatty acid composition of *Pistacia atlantica* fruit oil

Fatty acid	% Area
Palmitoleic acid C 16:1	1.84 ± 0.11
Palmitic acid C 16:0	11.86 ± 0.19
Linoleic acid C 18:2	37.44 ± 0.30
Oleic acid C 18:1	46.18 ± 0.72
linolenic acid C 18:3	0.09 ± 0.01
stearic acid C 18:0	2.61 ± 0.15
SFA	14.47
MUFA	48.02
PUFA	37.51

Fatty Acid Composition of PAO

PAO s highly valued for its rich composition of fatty acids, contributing to its diverse applications in culinary, cosmetic, and nutritional fields. The predominant fatty acids in PAO are oleic acid (approximately 40-60%), linoleic acid (about 20-30%), and palmitic acid (around 5-10%). Additionally, PAO contains smaller proportions of stearic, linolenic, and arachidonic acids. The fatty acid composition of PAO is influenced by factors such as the plant's geographic origin and the oil extraction method, both of which affect its final profile. This variability enables PAO to serve multiple purposes, including its use as a nutritious oil in food products, a moisturizing and anti-aging agent in cosmetics, and as a potential health supplement supporting cardiovascular health, owing to its high unsaturated fatty acid content [5, 36].

Table 3 presents the fatty acid composition of *P. atlantica* oil (PAO) as a percentage of the total area for each fatty acid. The major components include oleic acid (C18:1) at 46.18%, linoleic acid (C18:2) at 37.44%, and palmitic acid (C16:0) at 11.86%. Minor constituents are palmitoleic acid (C16:1) at 1.84%, stearic acid (C18:0) at 2.61%, and linolenic acid (C18:3) at 0.09%. The oil's fatty acid profile is dominated by monounsaturated fatty acids (MUFAs) at 48.02%, followed by polyunsaturated fatty acids (PUFAs) at 37.51%, with saturated fatty acids (SFAs) making up the smallest proportion at

14.47%. Oleic, linoleic, and linolenic acids contribute to improved skin hydration and regeneration due to their moisturizing and anti-inflammatory properties, which also help reduce inflammation and aid wound healing. Palmitic acid enhances skin protection and hydration, while palmitoleic acid offers antimicrobial properties and supports skin elasticity. Stearic acid stabilizes formulations and enhances moisturizing effects. The dominance of monounsaturated and polyunsaturated fatty acids highlights their significant potential for promoting healthy skin and supporting effective wound recovery [37].

Characterization of CNP

Oil-in-water nanoemulsions (NEs) derived from cold-pressed *Pistacia atlantica* fruit oil (NEP) were prepared using high-energy methods. These nanoemulsions were further encapsulated with chitosan cross-linked by tripolyphosphate (TPP) using the ionic gelation method to form chitosan nanocapsules (CNP). Figures 1A and 1B illustrate the mean droplet diameter and polydispersity index (PDI) for NEP and CNP, respectively. The PDI measures the size distribution of droplets, with values below 0.5 indicating relatively homogeneous distributions.

The mean droplet size for NEP (Figure 1A) was 89.75 nm, ranging from 74.87 nm to 107.45 nm, with a standard deviation (SD) of 12.86 nm. This range reflects a moderately diverse particle population. In contrast, the mean size of CNP (Figure 1B) was slightly larger at 104.76 nm, with a range of 89.58 nm to 122.32 nm and an SD of 12.42 nm. These results confirm that while both formulations fall within the nanoscale, the nanocapsules have slightly larger particles compared to the nanoemulsions.

a

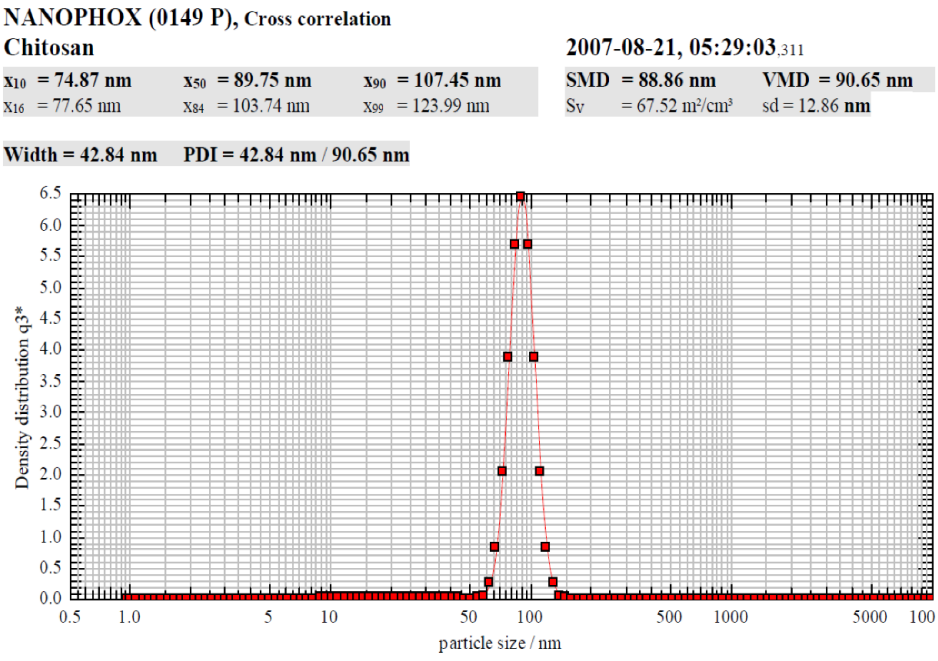

b

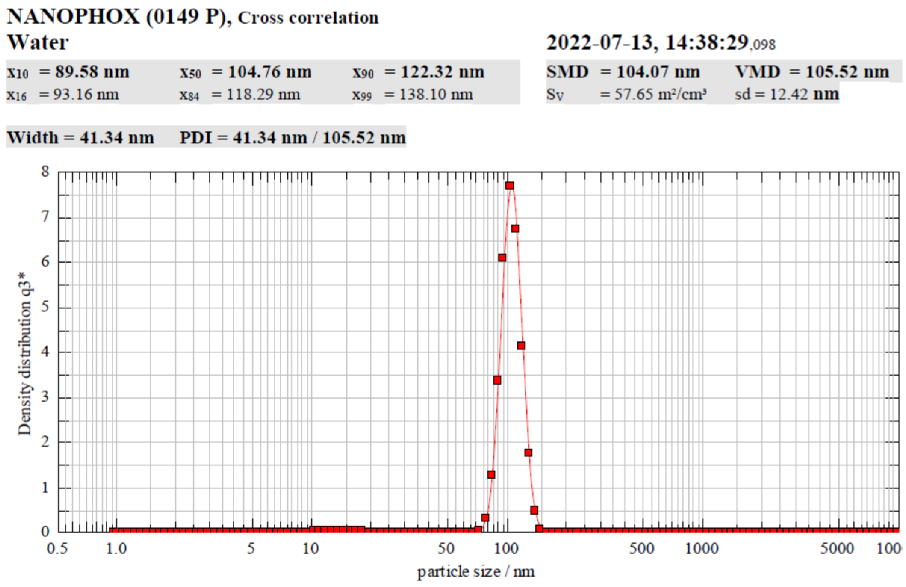

Fig. 1 DLS analysis shows the mean hydrodynamic size and polydispersity index of the nanoemulsion (a) and nanocapsule (b) of PAO.

The PDI values were calculated as 0.42 for NEP and 0.41 for CNP, both indicating relatively narrow particle size distributions and suggesting good uniformity in each formulation. However, the nanoemulsion displayed a marginally broader size range compared to the nanocapsules. This data underscores the effectiveness of both formulations in achieving nanoscale particle sizes with minimal variability.

The differences in mean particle size and PDI between the nanoemulsion and the nanocapsules suggest that the encapsulation process affects the overall size of the particles. The increase in mean size observed in the nanocapsules could imply enhanced encapsulation efficacy or aggregation tendencies, potentially due to the added complexity of their structural formulation. Therefore, both formulations appear to be suitable for applications in drug delivery and formulation science. However, polymeric encapsulation enhances physical stability, provides chemical protection against environmental factors, and improves the bioavailability of poorly soluble compounds more effectively than nanoemulsions.

Fabrication and Morphology of PCP NFs

The scanning electron microscopy (SEM) images in Figure 2 provide insights into the influence of chitosan nanocapsules containing *Pistacia atlantica* oil (PAO) on the formation and morphology of the nanofibers across formulations A through D. Formulation A, without chitosan nanocapsules, exhibits a uniform nanofiber structure with consistent diameters.

As chitosan nanocapsules were added to formulation B, a noticeable change in fiber morphology was observed. The nanofibers displayed slight variations in diameter and the presence of occasional beading, which can be attributed to the addition of CNPs to the spinning solution. The narrower size distribution seen in the histogram indicates a more homogeneous fiber formation and a decrease in fiber diameter, likely due to the increase in the solution's conductivity, which is influenced by the surface charge of the nanocapsules.

Further increasing the chitosan nanocapsule content in formulation C resulted in more pronounced changes in the nanofiber structure. The fibers exhibited slightly smaller diameter variations, with more extensive beading. This morphological transformation can be associated with the significantly higher viscosity, along with the increased electric charge of the spinning solution, which can disrupt the electrospinning process and lead to the formation of a less uniform fiber network. The histogram for formulation C reflects this increased heterogeneity, with a nearly constant size distribution. This suggests that despite the approximately constant diameter of the nanofibers, the presence of nanocapsules inside the polymer fibers and their accumulation in certain areas contributes to unevenness along the nanofibers.

The most profound changes were observed in formulation D, where the high concentration of chitosan nanocapsules led to the formation of thick, irregular fibers with extensive beading. This dramatic alteration in fiber morphology suggests that the nanocapsules are now exerting a dominant influence on the electrospinning dynamics, potentially affecting parameters such as electrical conductivity and surface tension. The histogram for formulation D exhibits a marked increase in fiber diameter variability, indicating the challenges in maintaining consistent nanofiber formation at these higher nanocapsule concentrations. Examination of the SEM and distribution of PCP 2 in Figure 2D shows that the chitosan-TPP nanocapsules within the solution lead to variability in fiber diameter. Areas with higher nanocapsule concentration produce slightly thicker segments within the fiber, while increasing the electrical charge of the polymer solution reduces the diameter of most of the nanofibers.

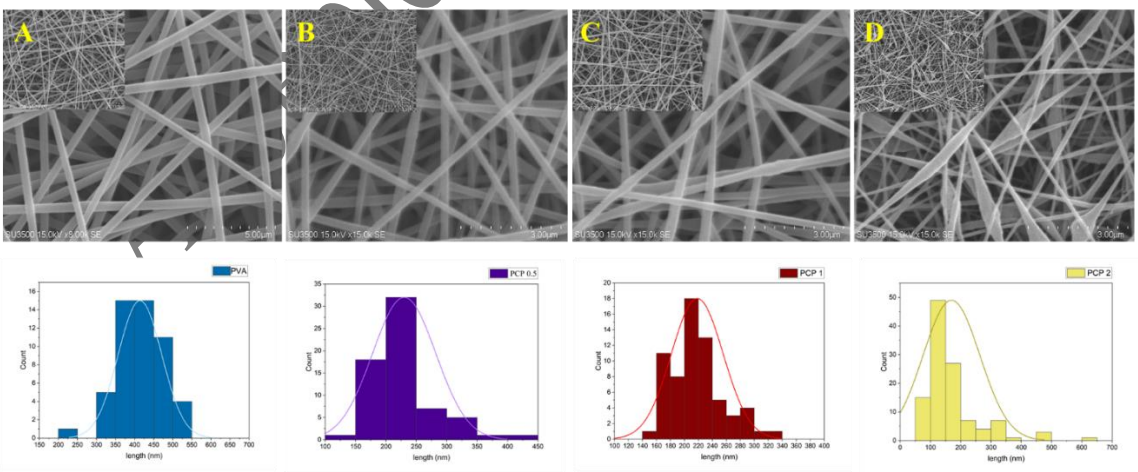

Fig. 2 SEM images and corresponding histograms showing the diameter distribution of (a) PVA nanofibers, (b) PCP0.5, (c) PCP1, and (d) PCP2.

The progressive changes in nanofiber morphology and size distribution from formulation A to D are directly attributed to the increasing content of chitosan nanocapsules containing PAO. While lower nanocapsule concentrations (B) allow for the production of uniform fibers, higher concentrations (D) introduce greater complexity in the fiber structure, driven by enhanced conductivity, viscosity, and altered electrospinning behavior. This understanding suggests that the optimal

nanocapsule-to-polymer ratio for achieving the desired nanofiber properties for controlled drug delivery and wound dressing applications is 1:1 CNP to PVA.

Evaluation of Encapsulation Efficiency and Loading Capacity

The encapsulation efficiency (% EE) and loading capacity (% LC) of *Pistacia atlantica* oil (PAO) were evaluated for three formulations: PCP 0.5, PCP 1, and PCP 2. These formulations correspond to polyvinyl alcohol (PVA) to chitosan nanocapsule (CNP) ratios of 0.5:1, 1:1, and 1:2, respectively. Figure 3 reveals that while the encapsulation efficiency remains relatively constant, the loading capacity increases significantly as the CNP content rises. Specifically, the % EE for PCP 0.5 was 76.9%, while both PCP 1 and PCP 2 exhibited an EE of 81.3%. The consistent EE values for PCP 1 and PCP 2 highlight that the encapsulation of *Pistacia atlantica* oil occurs primarily during the preparation of the chitosan nanocapsules (CNP) and is not further influenced by the electrospinning process with PVA. This indicates that the integration of CNP into the PVA nanofiber matrix does not alter the encapsulation efficiency, as the electrospinning process does not affect the oil's pre-established encapsulation.

In contrast, the loading capacity (% LC) increased significantly with higher CNP content. PCP 0.5 had an LC of 14.2%, which increased to 21.62% for PCP 1 and reached 32.37% for PCP 2. This trend reflects that increasing the CNP concentration leads to a greater amount of oil and chitosan being incorporated within the same PVA matrix. Therefore, while the EE remains unchanged, the higher CNP content enhances the LC, which is crucial for applications that require a higher payload of bioactive compounds for effective skin care and wound healing treatments.

These results suggest that adjusting the PVA to CNP ratio is an effective strategy for modulating the loading capacity of the nanofibers without compromising encapsulation efficiency. The constant EE emphasizes that the primary encapsulation of *P. atlantica* oil is governed by the initial preparation of CNP, and subsequent incorporation into PVA nanofibers serves mainly to embed the nanocapsules rather than alter the oil encapsulation.

PAO Delivery

Figure 4 displays the release profiles of nanocomposite fibers (PCP 0.5, PCP 1, and PCP 2) at two different pH levels: acidic (pH 5.5, panel A) and neutral (pH 7.4, panel B). In both pH conditions, PCP 0.5 demonstrates the highest release rate, followed by PCP 1, with PCP 2 showing the slowest release over time. At pH 7.4, the overall release rates for all samples are faster compared to pH 5.5, indicating pH-dependent release behavior, where neutral conditions enhance the release rate. The differences in release profiles suggest that the formulation composition influences the release dynamics, with higher CNP concentrations likely contributing to slower, more controlled release, particularly in acidic conditions. This pH-sensitive behavior highlights the potential for these samples to achieve targeted release in environments with specific pH values.

Chitosan, a natural polysaccharide with amino groups, can interact with PVA through hydrogen bonding, while TPP acts as a crosslinking agent that further stabilizes the chitosan structure. When combined with PVA, chitosan-TPP nanocapsules can enhance the crosslinking within the nanofiber matrix, improving mechanical strength, stability, and water resistance. This crosslinking effect is beneficial for applications requiring sustained release, as it can slow the dissolution rate of PVA in aqueous environments, providing a more controlled release profile of encapsulated compounds.

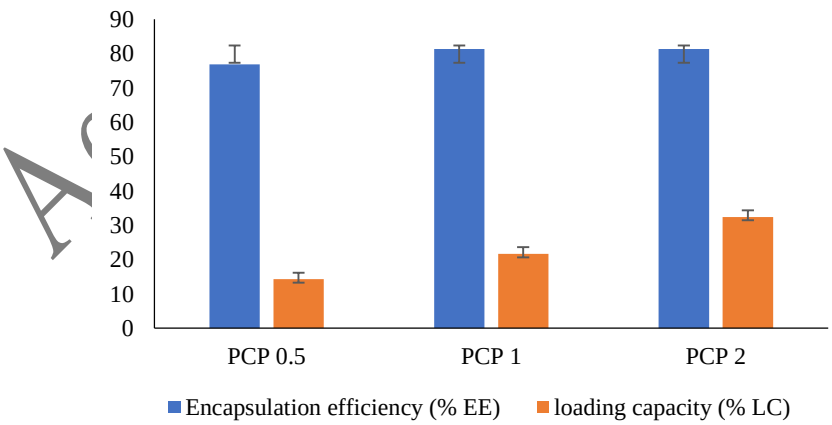

Fig. 3 The encapsulation efficiency (EE) and loading capacity (LC) of PAO loaded nanofibers by different CNP content

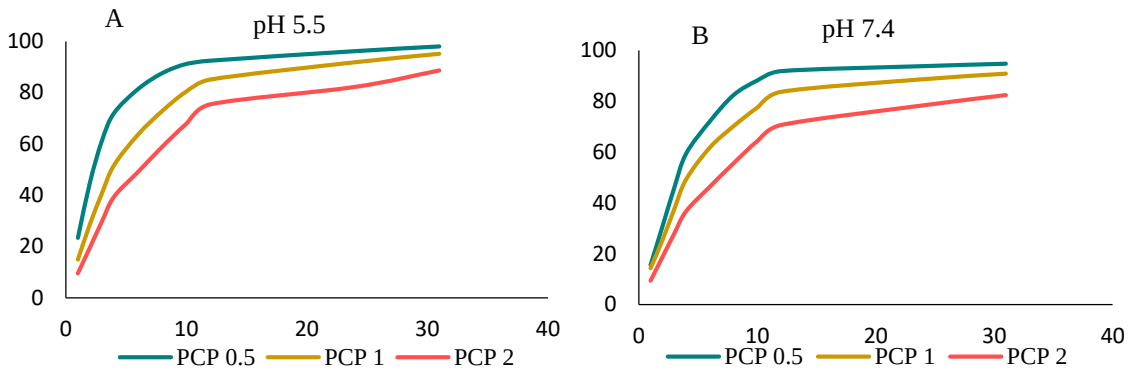

Fig. 4 Cumulative percentage PAO release profiles for three samples (PCP0.5, PCP1, and PCP2) at pH 5.5 (A) and pH 7.4 (B).

These nanofibers could be suitable for skin care and wound healing applications, especially given their controlled, pH-dependent release behavior. Infected wounds often have a slightly more acidic environment due to bacterial metabolism, which can lower the local pH. This makes the slower release of samples like PCP 1 and PCP 2 at acidic pH (5.5) particularly beneficial, as they can provide a sustained delivery of active compounds over time, potentially enhancing antimicrobial effectiveness and reducing the need for frequent reapplication.

For infected wounds, PCP 2 may be the most advantageous choice, as its slower release profile at pH 5.5 allows for prolonged exposure to the active agents, which could help manage bacterial load and inflammation over an extended period. This sustained release can support continuous therapeutic effects, making it ideal for managing infections where constant, controlled delivery of antimicrobial or healing agents is beneficial.

Antioxidant Activity of NFs

We investigated the antioxidant activity of various samples using the DPPH and FRAP assays, as shown in Table 4. The FRAP assay results, expressed as µmol ESF/100g, revealed that PAO had the highest antioxidant activity (200.7 ± 4.2 µmol ESF/100g), while pure PVA nanofibers showed a low value (14.6 ± 0.9 µmol ESF/100g). The CNP film with PAO exhibited improved antioxidant activity (25.1 ± 0.8 µmol ESF/100g), and the PCP samples showed a progressive increase in FRAP values: PCP 0.5 (44.9 ± 1.5 µmol ESF/100g), PCP 1 (58.4 ± 1.3 µmol ESF/100g), and PCP 2 (79.4 ± 2.1 µmol ESF/100g), suggesting that higher CNP concentrations enhance reducing power.

Table 4 Antioxidant activity of encapsulated PAO in nanofibers by FRAP and DPPH assay.

Sample	Antioxidant activity	
	FRAP assay *(µmol ESF/100g)*	DPPH• IC_{50} *(µg/ml)*
BHT	–	11.64
PAO	–	231.23
PAF	*200.7 ± 4.2*	–
PVA nanofiber	14.6 ± 0.9	82013
CNP dried film	25.1 ± 0.8	12350
PCP 0.5	44.9 ± 1.5	20711
PCP 1	58.4 ± 1.3	9793.6
PCP 2	79.4 ± 2.1	7344.7

In the DPPH assay, BHT (positive control) had an IC_{50} of 11.64 µg/mL, while PAO alone showed an IC_{50} of 231.23 µg/mL. Pure PVA nanofibers had an IC_{50} of 82,013 µg/mL. PAO in the CNP film improved radical scavenging, reducing the IC_{50} to 12,350 µg/mL. The PCP samples showed progressively improved scavenging activity with decreasing IC_{50} values: PCP 0.5 (20,711 µg/mL), PCP 1 (9,793.6 µg/mL), and PCP 2 (7,344.7 µg/mL), indicating enhanced antioxidant potential with higher PAO and chitosan concentrations.

These results show that integrating PAO into PVA nanofibers significantly enhances antioxidant activity. The higher the PAO and chitosan content, the stronger the antioxidant potential, suggesting promising applications in biomedical, cosmetic, and food packaging industries.

ATR – FTIR of NFs

The ATR-FTIR spectra presented in Figure 5 reveal the characteristic peaks of various formulations, including chitosan nanocapsules (CNP), pure PVA nanofibers, and PVA nanofibers with varying CNP ratios (1:1 for PCP1 and 2:1 for PCP2). These spectra provide valuable insights into the chemical composition and interactions within the formulations.

The CNP spectrum (orange) exhibits distinctive peaks corresponding to *P. atlantica* oil and the chitosan-TPP encapsulation. A strong band around 1740 cm^{-1} corresponds to the C=O stretching in ester groups of fatty acids within the oil. Additionally,

a broad band in the 3200–3400 cm^{-1} region is observed, which is attributed to O-H stretching in chitosan and potential hydrogen bonding. Peaks around 1140–1200 cm^{-1} (marked by a gray circle) likely indicate the P=O stretching of TPP, confirming successful crosslinking between chitosan and TPP.

In the spectra of PVA, PCP1, and PCP2, distinct differences are observed, reflecting the increasing CNP content. The PVA nanofiber spectrum shows characteristic peaks of PVA, including the O-H stretching band around 3300 cm^{-1} and C-O stretching in the 1050–1150 cm^{-1} region (orange strip). These peaks persist in the PCP1 and PCP2 spectra, albeit with modifications. In PCP1, the incorporation of 50% CNP introduces new bands and broadening in the 2800–3000 cm^{-1} range, corresponding to C-H stretching of the fatty acid chains in *P. atlantica* oil. Additionally, a slightly more pronounced peak around 1740 cm^{-1} indicates the presence of ester groups in the oil.

In PCP2, where the CNP content doubles, the peaks associated with PAO, particularly the C=O stretching at 1740 cm^{-1} and the C-H stretching in the 2800–3000 cm^{-1} region (purple bar), become more prominent, confirming a higher PAO content. Furthermore, the broad O-H stretching around 3300 cm^{-1} (green bar), linked to both PVA and chitosan, becomes more intense, indicating potential interactions between PVA and the chitosan-TPP nanocapsules.

Cell Viability Assay

The evaluation of human dermal fibroblast (HDF) cell viability via the MTT assay is a useful initial test to assess the biocompatibility and cytotoxicity of materials intended for skin care and wound healing applications. Fibroblast cells play a critical role in collagen synthesis, wound repair, and the overall maintenance of skin structure and functionsults indicate that the compounds did not significantly affect HDF cell viability or proliferation, demonstrating minimal cytotoxicity. Figure 6 shows that at the lowest concentration (62.5 µg/mL), all samples maintained high cell viability, with CNP showing the highest viability (~95%) due to the bioactive properties of *P. atlantica* oil. PVA exhibited ~89% viability, while PCP demonstrated slightly lower viability (~82%).

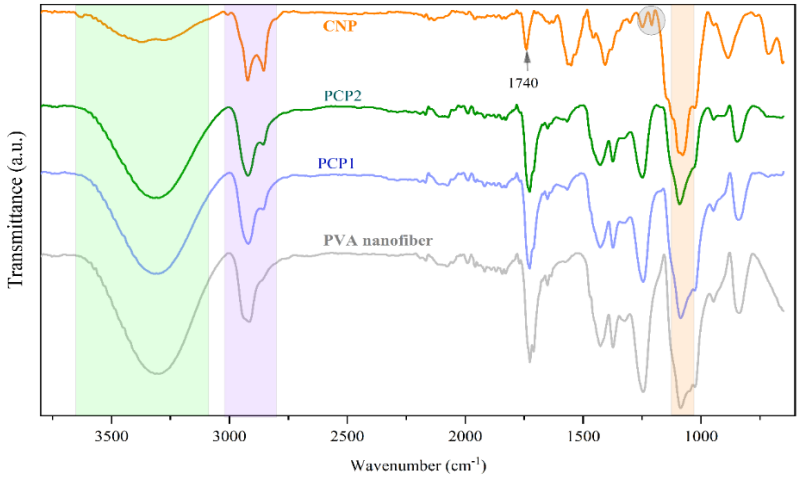

Fig. 5 ATR FTIR spectra of pure PVA nanofiber, chitosan nanocapsule of PAO (CNP), PCP1 and PCP2 nanofibers by 1:1 and 1:2 ratio to PVA to CNP, respectively.

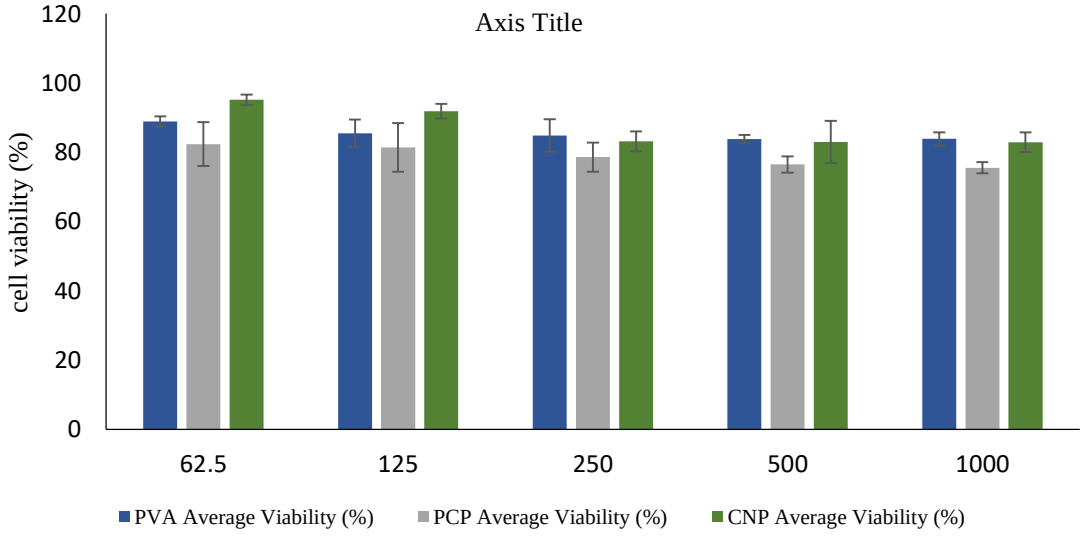

Fig. 6 Human Dermal Fibroblasts (HDFs) cell viability assay for pure PVA nanofibers, CNP, and PCP at increasing concentrations (62.5, 125, 250, 500, and 1000 µg/mL).

As concentration increased, CNP consistently exhibited higher viability (above 82%) compared to PCP and PVA, which decreased to ~76% and ~83%, respectively. This suggests that CNP's encapsulated oil provides a protective bioactive environment, while the PVA matrix in PCP may slightly affect cell response.
Overall, CNP demonstrated the best biocompatibility, making it ideal for sustained bioactivity. In contrast, PCP offers a balance of structural support and bioactivity, making it suitable for skin care and wound healing applications.

CONCLUSION

In this study, a nanocomposite system was created by encapsulating *P. atlantica* oil (PAO) within chitosan nanocapsules, which were subsequently integrated into polyvinyl alcohol (PVA) nanofibers using electrospinning. The resulting formulation exhibited excellent encapsulation efficiency and notable loading capacity, attributed to the uniform dispersion of nanocapsules within the PVA matrix. These findings underscore the effectiveness of electrospinning for fabricating stable, oil-infused nanofibers. The encapsulated PAO preserved its antioxidant properties, which are crucial for biomedical applications aimed at combating oxidative stress. The chitosan-based matrix effectively maintained the bioactivity of PAO, ensuring its sustained efficacy. Furthermore, the release profile of PAO from the nanofiber composite exhibited a controlled, sustained release, indicating its suitability for applications requiring prolonged therapeutic effects. Cytocompatibility tests with human dermal fibroblasts (HDFs) revealed excellent cell viability, particularly in formulations containing PAO, suggesting good biocompatibility and favorable cellular responses. These findings indicate the potential of this nanocomposite for wound healing and tissue regeneration applications. Overall, the results demonstrate the multifunctional potential of chitosan nanocapsules embedded in PVA nanofibers, offering enhanced antioxidant activity, efficient encapsulation, and controlled release, with significant prospects for biomedical and pharmaceutical applications.

Conflict of Interests

The authors have not declared any conflict of interests.

ACKNOWLEDGEMENT

We would like to express our gratitude to the Shahid Beheshti University Research Council for their infrastructure support.

REFERENCES

1. Cedillo-Cortezano M., Martinez-Cuevas L.R., López J.A.M., Barrera López I.L., Escutia-Perez S., Petricevich V.L. Use of Medicinal Plants in the Process of Wound Healing: A Literature Review. Pharm. 2024;17(3):303.
2. Fernandes A., Rodrigues P.M., Pintado M., Tavaria F.K. A systematic review of natural products for skin applications: Targeting inflammation, wound healing, and photo-aging. Phytomedicine. 2023;115:154824.
3. Farhan M. The Promising Role of Polyphenols in Skin Disorders. Mol. 2024;29(4):865.
4. Benmohamed M., Guenane H., Messaoudi M., Zahnit W., Egbuna C., Sharifi-Rad M., Chouh A., Seghir B.B., Rebiai A., Boubekeur S., Azli T., Harrat M., Sawicka B., Atanassova M., Yousfi M. Mineral Profile, Antioxidant, Anti-Inflammatory, Antibacterial, Anti-Urease and Anti-α-Amylase Activities of the Unripe Fruit Extracts of Pistacia atlantica. Mol. 2023;28(1).
5. Bozorgi M., Memariani Z., Mobli M., Salehi Surmaghi M.H., Shams-Ardekani M.R., Rahimi R. Five Pistacia species (P. vera, P. atlantica, P. terebinthus, P. khinjuk, and P. lentiscus): A Review of Their Traditional Uses, Phytochemistry, and Pharmacology. The Sci World J. 2013;2013(1):219815.
6. Mahjoub F., Akhavan Rezayat K., Yousefi M., Mohebbi M., Salari R. Pistacia atlantica Desf. A review of its traditional uses, phytochemicals and pharmacology. J Med Life. 2018;11(3):180-86.
7. Memariani Z., Sharifzadeh M., Bozorgi M., Hajimahmoodi M., Farzaei M.H., Gholami M., Siavoshi F., Saniee P. Protective effect of essential oil of Pistacia atlantica Desf. on peptic ulcer: Role of α-pinene. J Traditional Chinese Med. 2017;37(1):57-63.
8. Hamidi S.A., Tabatabaei Naeini A., Oryan A., Tabandeh M.R., Tanideh N., Nazifi S. Cutaneous Wound Healing after Topical Application of Pistacia atlantica Gel Formulation in Rats. Turk J Pharm Sci. 2017;14(1):65-74.
9. Fadilah N.I.M., Phang S.J., Kamaruzaman N., Salleh A., Zawani M., Sanyal A., Maarof M., Fauzi M.B. Antioxidant Biomaterials in Cutaneous Wound Healing and Tissue Regeneration: A Critical Review. Antioxidants. 2023;12(4):787.
10. Saber-Tehrani M., Givianrad M.H., Aberoomand-Azar P., Waqif-Husain S., Jafari Mohammadi S.A. Chemical Composition of Iran's Pistacia atlantica Cold-Pressed Oil. J Chem. 2013;2013:126106.
11. Najafiasl M., Osfouri S., Zaeri S. Evaluation of physicochemical properties, release kinetics, and in vitro/in vivo wound healing activity of the electrospun nanofibres loaded with the natural antioxidant oil from Pistacia atlantica. J Drug Delivery Sci Technol. 2023;84:104512.
12. El Zerey-Belaskri A., Belyagoubi-Benhammou N., Benhassaini H. From traditional knowledge to modern formulation: potential and prospects of Pistacia atlantica desf. essential and fixed oils uses in cosmetics. Cosmet. 2022;9(6):109.
13. Rauf A., Patel S., Uddin G., Siddiqui B.S., Ahmad B., Muhammad N., Mabkhot Y.N., Hadda T.B. Phytochemical, ethnomedicinal uses and pharmacological profile of genus Pistacia. Biomedicine and Pharmacotherapy. 2017;86:393-404.
14. Carvalho I.T., Estevinho B.N., Santos L. Application of microencapsulated essential oils in cosmetic and personal healthcare products – a review. Int J Cosmet Sci. 2016;38(2):109-19.
15. Yammine J., Chihib N.-E., Gharsallaoui A., Ismail A., Karam L. Advances in essential oils encapsulation: Development, characterization and release mechanisms. Poly Bull. 2024;81(5):3837-82.

16. Reis D.R., Ambrosi A., Luccio M.D. Encapsulated essential oils: A perspective in food preservation. Future Foods. 2022;5:100126.
17. Maes C., Bouquillon S., Fauconnier M.L. Encapsulation of Essential Oils for the Development of Biosourced Pesticides with Controlled Release: A Review. Mol. 2019;24(14).
18. Cimino C., Maurel O.M., Musumeci T., Bonaccorso A., Drago F., Souto E.M.B., Pignatello R., Carbone C. Essential Oils: Pharmaceutical Applications and Encapsulation Strategies into Lipid-Based Delivery Systems. Pharm. 2021;13(3).
19. Vinceković M., Jurić S., Marijan M., Viskić M., Vlahoviček-Kahlina K., Maslov Bandić L. Encapsulation of herb extracts (Aromatic and medicinal herbs). 2021; 263-322.
20. Taouzinet L., Djaoudene O., Fatmi S., Bouiche C., Amrane-Abider M., Bougherra H., Rezgui F., Madani K. Trends of nanoencapsulation strategy for natural compounds in the food industry. Processes. 2023;11(5):1459.
21. Salvioni L., Morelli L., Ochoa E., Labra M., Fiandra L., Palugan L., Prosperi D., Colombo M. The emerging role of nanotechnology in skincare. Adv in Colloid and Interface Sci. 2021;293:102437.
22. Stoyanova N., Nachev N., Spasova M. Innovative bioactive nanofibrous materials combining medicinal and aromatic plant extracts and electrospinning method. Membr. 2023;13(10):840.
23. Zahmatkeshan M., Adel M., Bahrami S., Esmaeili F., Rezayat S.M., Saeedi Y., Mehravi B., Jameie S.B., Ashtari K. Polymer Based Nanofibers: Preparation, Fabrication, and Applications. In Barhoum A Bechelany M, Makhlouf A (Eds.), Handbook of Nanofibers (pp. 1-47). Cham: Springer Int Publ. 2018.
24. Oliveira C., Sousa D., Teixeira J.A., Ferreira-Santos P., Botelho C.M. Polymeric biomaterials for wound healing. [Review]. Fron in Bioeng Biotechnol. 2023;11.
25. Shalaby M.A., Anwar M.M., Saeed H. Nanomaterials for application in wound Healing: Current state-of-the-art and future perspectives. J Polym Res. 2022;29(3):91.
26. Iacob A.-T., Drăgan M., Ionescu O.-M., Profire L., Ficai A., Andronescu E., Confederat L.G., Lupaşcu D. An overview of biopolymeric electrospun nanofibers based on polysaccharides for wound healing management. Pharm. 2020;12(10):983.
27. International A., international A.o.o.a.c., Horwitz W., Latimer e., Latimer G.W. Official Methods of Analysis of AOAC International: AOAC Int. 2012.
28. Fathi F., Ebrahimi S.N., Valadão A.I.G., Andrade N., Costa A.S.G., Silva C., Fathi A., Salehi P., Martel F., Alves R.C., Oliveira M.B.P.P. Exploring Gunnera tinctoria: From Nutritional and Anti-Tumoral Properties to Phytosome Development Following Structural Arrangement Based on Molecular Docking. Mol. 2021;26(19):5935.
29. Özcan M.M., Ghafoor K., Al Juhaimi F., Ahmed I.A.M., Babiker E.E. Effect of cold-press and soxhlet extraction on fatty acids, tocopherols and sterol contents of the Moringa seed oils. South African J Bot. 2019;124:333-37.
30. Hameed M., Rasul A., Waqas M.K., Saadullah M., Aslam N., Abbas G., Latif S., Afzal H., Inam S., Akhtar Shah P. Formulation and Evaluation of a Clove Oil-Encapsulated Nanofiber Formulation for Effective Wound-Healing. Mol. 2021;26(9):2491.
31. Mahdavinia G.R., Mosallanezhad A., Soleymani M., Sabzi M. Magnetic- and pH-responsive κ-carrageenan/chitosan complexes for controlled release of methotrexate anticancer drug. Int J Biol Macromol. 2017;97:209-17.
32. Baliyan S., Mukherjee R., Priyadarshini A., Vibhuti A., Gupta A., Pandey R.P., Chang C.-M. Determination of Antioxidants by DPPH Radical Scavenging Activity and Quantitative Phytochemical Analysis of Ficus religiosa. Mol. 2022;27(4):1326.
33. Benzie I.F.F., Strain J.J. The Ferric Reducing Ability of Plasma (FRAP) as a Measure of "Antioxidant Power": The FRAP Assay. Anal Biochem. 1996;239(1):70-76.
34. Ros E. Health Benefits of Nut Consumption. Nutr. 2010;2(7):652-82.
35. Poljšak N., Kreft S., Kočevar Glavač N. Vegetable butters and oils in skin wound healing: Scientific evidence for new opportunities in dermatology. Phytotherapy Res. 2020;34(2):254-69.
36. Hazrati S., Govahi M., Ebadi M.-T., Habibzadeh F. Comparison and evaluation of oil content, composition and antioxidant properties of Pistacia atlantica and Pistacia khinjuk grown as wild. Int J Hortic Sci Technol. 2020;7(2):165-74.
37. Jara C.P., Mendes N.F., Prado T.P.d., de Araújo E.P. Bioactive Fatty Acids in the Resolution of Chronic Inflammation in Skin Wounds. Adv in WND Care. 2020;9(8):472-90.